Steady-State Dynamics and Effective Temperature for a Model of Quantum Criticality in an Open System

P. Ribeiro
Russian Quantum Center, Novaya street 100 A, Skolkovo, Moscow area, 143025 Russia
and CeFEMA, Instituto Superior Técnico, Universidade de Lisboa Avenida Rovisco Pais, 1049-001 Lisboa, Portugal

F. Zamani
Max Planck Institute for Physics of Complex Systems, 01187 Dresden, Germany
and Max Planck Institute for Chemical Physics of Solids, 01187 Dresden, Germany

S. Kirchner*
Center for Correlated Matter, Zhejiang University, Hangzhou, Zhejiang 310058, China
(Received 3 April 2015; revised manuscript received 2 September 2015; published 25 November 2015)

We study the thermal and nonthermal steady-state scaling functions and the steady-state dynamics of a model of local quantum criticality. The model we consider, i.e., the pseudogap Kondo model, allows us to study the concept of effective temperatures near fully interacting as well as weak-coupling fixed points. In the vicinity of each fixed point we establish the existence of an effective temperature—different at each fixed point—such that the equilibrium fluctuation-dissipation theorem is recovered. Most notably, steady-state scaling functions in terms of the effective temperatures coincide with the equilibrium scaling functions. This result extends to higher correlation functions as is explicitly demonstrated for the Kondo singlet strength. The nonlinear charge transport is also studied and analyzed in terms of the effective temperature.

DOI: 10.1103/PhysRevLett.115.220602 PACS numbers: 05.70.Ln, 05.70.Jk, 64.70.Tg, 72.10.Fk

The interest in understanding the dynamics of strongly correlated systems beyond the linear response regime has in recent years grown tremendously. The quantum dynamics in adiabatically isolated optical traps has been successfully modeled using powerful numerical schemes [1,2]. In open systems mainly diagrammatic techniques on the Schwinger-Keldysh contour have been employed. For nanostructured systems several techniques exist to describe the ensuing out-of-equilibrium properties. These approaches, however, are either perturbative in nature [3], centered around high temperatures and short times [4–8], or approximate the continuous baths by discrete Wilson chains [9–11]. The situation might be simpler for nonlinear dynamics that arises in the vicinity of a quantum critical point (QCP), where a vanishing energy scale leads to scaling and universality [12–19].

For the dynamics near classical continuous phase transitions a well-established theoretical framework exists, tying the dynamics to the statics and the conserved quantities [20]. In addition, the concept of effective temperature ($T_{\rm eff}$) was established as a useful notion for the relaxational dynamics of classical critical systems [21–24], although it appears somewhat less useful for fully interacting critical points [23]. $T_{\rm eff}$ is commonly defined by extending the equilibrium fluctuation-dissipation theorem to the nonlinear regime. The existence of effective temperature in quantum systems was recently investigated [18,25–28]. For a recent review see Ref. [25]. In comparison to classical criticality, at a QCP, dynamics already enters at the equilibrium level. For a QCP that can be described by a Ginzburg-Landau-Wilson functional in elevated dimensions, it was found that the voltage-driven transition is in the universality class of the associated thermal classical model with voltage acting as $T_{\rm eff}$ [12]. Unconventional QCPs in contrast are not described solely in terms of an order parameter functional [29,30].

In this Letter we address the following general questions within a model system of unconventional quantum criticality. Is the existence of $T_{\rm eff}$ tied to dynamical (or ω/T) scaling? Does $T_{\rm eff}$ have meaning for higher correlation functions? How unique is $T_{\rm eff}$ at a given fixed point once boundary conditions have been specified? Can critical scaling functions be expressed through $T_{\rm eff}$ and if so, how do these scaling functions relate to the equilibrium scaling functions? The model system is the pseudogap Kondo model (PKM) that describes a quantum spin antiferromagnetically coupled to a conduction electron bath possessing a pseudogap near its Fermi energy, characterized by a power-law exponent. Depending on the coupling strength, the quantum spin is either screened or remains free in the zero temperature (T) limit. The two phases are separated by a critical point displaying critical Kondo destruction, see Fig. 1. The PKM has been invoked to describe nonmagnetic impurities in the cuprate superconductors [31] and point defects in graphene [32]. It underlies the pseudogap free moment phases occurring in certain disordered metals [33] and can also be realized in

double quantum-dot systems [34]. The quantum critical properties of the PKM in equilibrium have been addressed in Refs. [35–45]. Our main findings are that the steady-state dynamic spin susceptibility, the conductance, and the Kondo-singlet strength, a four-point correlator, reproduce their equilibrium behavior in the scaling regimes of the fixed points of the model when expressed in terms of a fixed-point specific $T_{\rm eff}$.

The model.—We consider a PKM with a density of states that vanishes in a power-law fashion with exponent $0 \le r \le 1$ at their Fermi levels, $\rho^{-}_{c,l}(\omega) \sim |\omega|^r \Theta(D - |\omega|)$, with half-bandwidth D. Here, $l = L, R$ labels the two leads, see Fig. 1(a). In the multichannel version of the model the spin degree of freedom ($\boldsymbol{S}$) is generalized from $SU(2)$ to $SU(N)$ and the fermionic excitations (c) of the leads transform under the fundamental representation of $SU(N) \times SU(M)$ with N spin and M charge channels. At $T = 0$ and $r < r_{\rm max} < 1$, a critical point (C) separates a multichannel Kondo (MCK)-screened phase from a local moment (LM) phase at a critical value J_c of the exchange coupling $J > 0$, see Fig. 1(b). The characterization of the phases and the leading power-law exponents of observables of the PKM have been obtained by perturbative renormalization group (RG), large-N methods, and numerical renormalization group (NRG) [35–38,40,43]. Within the large-N approach, at $T = 0$, scaling arguments are able to predict the critical exponents of dynamical observables [39,46]. Nonequilibrium steady states (NESSs) are obtained by applying a time-independent bias voltage $V = (\mu_L - \mu_R)/|e|$, where μ_l is the chemical potential of lead l, see Fig. 1(a). As T characterizes the fermionic reservoirs, it remains well defined even for $V \neq 0$.

A similar setup has been considered in a perturbative RG-like study adapted to the NESS condition [47]. This model has also been invoked in a variational study of the dynamics following a local quench where it was found that quenches in the Kondo phase thermalize while this is not the case for quenches across the QCP into the LM regime [48]. The system is described by the Hamiltonian

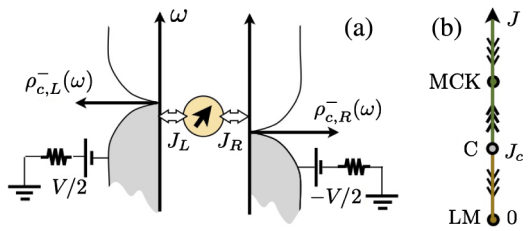

FIG. 1 (color online). (a) Sketch of the model: a spin interacts with two fermionic leads which are characterized by their respective density of states $\rho^{-}_{c,L/R}(\omega)$ and chemical potentials $\mu_{L/R}$. (b) Phase diagram of the multichannel PKM with gap exponent $r < r_{\rm max}$: A QCP (C) separates the multichannel Kondo (MCK) fixed point from the (weak-coupling) local moment (LM) fixed point.

$$H = \sum_{p\alpha\sigma l} \varepsilon_{pl} c^{\dagger}_{p\alpha\sigma l} c_{p\alpha\sigma l} + \frac{1}{N} \sum_{ll'} \sum_{\alpha} J_{ll'} \mathbf{S} \cdot \mathbf{s}_{\alpha;ll'}, \quad (1)$$

where $\sigma = 1, \ldots, N$ and $\alpha = 1, \ldots, M$ are, respectively, the $SU(N)$-spin and $SU(M)$-channel indices, l labels the leads and p is a momentum index. The cotunneling term [49] in Eq. (1) contains the local operators $\mathbf{s}^{i}_{\alpha;ll'} = \frac{1}{n_c} \sum_{pp'\sigma\sigma'} c^{\dagger}_{p\alpha\sigma l} t^{i}_{\sigma\sigma'} c^{\dagger}_{p'\alpha\sigma' l'}$ with t the fundamental representation of $SU(N)$ and n_c is the number of fermionic single-particle states. In a totally antisymmetric representation, one can decompose the spin operator as $S_{\sigma\sigma'} = f^{\dagger}_{\sigma} f_{\sigma'} - q\delta_{\sigma\sigma'}$, where q is subject to the constraint $\hat{Q} = \sum_{\sigma} f^{\dagger}_{\sigma} f_{\sigma} = qN$ and the $f^{\dagger}_{\sigma}, f_{\sigma'}$ obey fermionic commutation relations.

We employ a dynamical large-N limit [39,50], suitably generalized to the Keldysh contour [16,18] while keeping $q = (Q/N)$ and $\kappa = M/N$ constant. This results in

$$\Sigma^{>,<}_{B}(t) = i G^{>,<}_{f}(t) G^{<,>}_{c}(-t) \quad (2)$$

$$\Sigma^{>,<}_{f}(t) = -i\kappa G^{>,<}_{B}(t) G^{>,<}_{c}(t) \quad (3)$$

$$-i G^{<}_{f}(0) = q, \quad (4)$$

where G_f is the pseudofermion propagator and G_B is the propagator of a bosonic Hubbard-Stratonovich decoupling field. Σ_f (Σ_B) is the proper self-energy of G_f (G_B) and is related to it via the Dyson equation [51]. We assume that the exchange interaction originates from an Anderson-type model via a Schrieffer-Wolff transformation, so that a single coupling constant $J = J_L + J_R$ emerges [51]. For details on the numerics see Ref. [51]. In equilibrium, our approach yields dynamical scaling functions that coincide with those obtained from quantum Monte Carlo calculations [44].

Observables.—A possible order parameter for the transition from the overscreened Kondo to local-moment phase is given by $\lim_{T\to 0} T\chi(\omega = 0, T)$, where $\chi(\omega, T)$ is the Fourier transform of the local (impurity) spin-spin correlation function $\chi(t - t')$, see Fig. 2(a). We work on the Keldysh contour where the lesser and greater components are defined in the usual way as $\chi^{>}(t - t') = -i(1/N)\sum_a \langle S^a(t) S^a(t') \rangle$ with $t \in \gamma_{\leftarrow}$ and $t' \in \gamma_{\rightarrow}$ and $\chi^{<}(t - t') = -i(1/N)\sum_a \langle S^a(t') S^a(t) \rangle$, with $t \in \gamma_{\rightarrow}$ and $t' \in \gamma_{\leftarrow}$ so that $\chi^{R}(t) = \Theta(t)[\chi^{>}(t) - \chi^{<}(t)]$ and $\chi^{A} = \chi^{R} + \chi^{<} - \chi^{>}$. Here, $\gamma_{\rightarrow(\leftarrow)}$ is the forward (backward) branch of the Keldysh contour, respectively.

We also consider the "singlet-strength" ϕ_s, defined through the Kondo term contribution to the total energy of the system as $(1/N)\sum_{ll'} \sum_c J_{ll'} \langle \mathbf{S} \cdot \mathbf{s}_{c,ll'} \rangle = -J\kappa[(N^2 - 1)/N]\phi_s$ [52]. ϕ_s is a dimensionless quantity, which possesses a well-defined large-N limit and quantifies the degree of singlet formation. In terms of the fermionic fields, it can be written as the local-in-time limit of a four-point correlator [51]. Its equilibrium properties

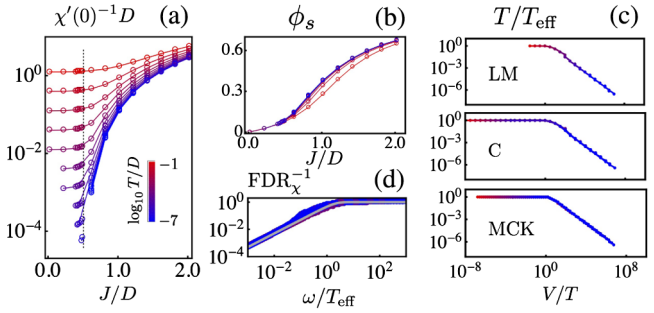

FIG. 2 (color online). (a) $\chi'(0)^{-1}$ vs J for different T. (b) ϕ_s vs J for different T. The $T=0$ curve is approached from below in the MCK and from above in the LM phases. (c) Scaling $T/T_{\rm eff}$ vs V/T at fixed points LM, C, and MCK: $T_{\rm eff}\sim V$ for $V\gg T$. (d) $\mathrm{FDR}_\chi^{-1}(\omega)$ vs $\omega/T_{\rm eff}$ near fixed point C, shown for $V/D=10^{-2},10^{-3},10^{-4},10^{-5},10^{-6}$. The grey line is $\mathrm{FDR}^{-1}(\omega)=\tanh(\beta\omega/2)$.

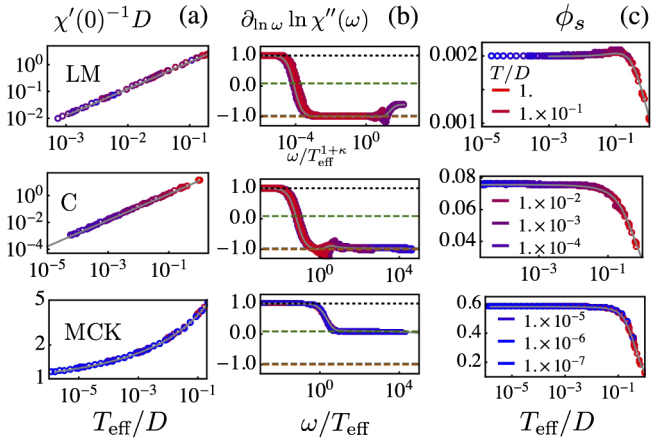

FIG. 3 (color online). Scaling of observables with $T_{\rm eff}$ at different fixed points for the values of V as in Fig. 2(d): (a) $\chi'(0)^{-1}$ vs $T_{\rm eff}$; (b) $\partial_{\ln\omega}\ln\chi''(\omega)$ vs $\omega/T_{\rm eff}$; (c) ϕ_s vs $T_{\rm eff}$. For each fixed point, the equilibrium scaling form (grey curves) is compared with the same quantity under nonequilibrium conditions and T substituted by $T_{\rm eff}$.

will be discussed below. The steady-state charge current passing through each channel is $\mathcal{J}_{\rm P}=-\partial_t\langle\hat{N}_L(t)\rangle/M$, where $\hat{N}_L=\sum_{p\alpha\sigma}c^\dagger_{p\alpha\sigma L}c_{p\alpha\sigma L}$ is the number of particles in the left lead. The out-of-equilibrium conditions considered here respect particle-hole symmetry which implies a vanishing energy current.

Throughout the Letter we set $\kappa=0.3$, $r=0.2$, and $q=1/2$. This results in $r_{\rm max}=0.412(4)$. Our choice of values for κ and r ensures a finite static spin susceptibility $\chi'(\omega=0)$ within the MCK phase as $T\to 0$. We denote the real (imaginary) part of $\chi^R(\omega)$ by χ' (χ'').

Thermal steady state.—The equilibrium ($V=0$) behavior of $\chi'(\omega=0,T)$ in the relaxational regime ($\omega\ll T$) near the MCK, C, and LM fixed points is shown in Fig. 2(a). For $J<J_c\simeq 0.44D$, i.e., in the LM phase, one observes Curie-like behavior at lowest temperatures $\chi'(\omega=0,T)\propto T^{-1}$. In the MCK phase ($J>J_c$ and with our choices of κ and r), the $T=0$ susceptibility remains finite. The grey lines in Fig. 3(b) show the scaling plots of the logarithmic derivative of $\chi''(\omega)$ for different values of the temperature, i.e., $\partial_{\ln\omega}\ln\chi''(\omega)$ for the different fixed points. Note that $\partial_{\ln\omega}\ln\chi''(\omega)\simeq\alpha_\chi$ within the scaling region where $\chi''(\omega)\propto|\omega|^{\alpha_\chi}$. The values of α_χ in the quantum coherent regime ($\omega/T\gg 1$) agree with those obtained analytically from a $T=0$ scaling ansatz [46] for the MCK ($\alpha_\chi\simeq 0.087$) and C ($\alpha_\chi=-0.97$) fixed points. These results are compatible with a dynamical scaling form $\chi''(\omega,T)=T^{\alpha_\chi}\Phi(\omega/T)$, in terms of an universal scaling function $\Phi(x)$ possessing asymptotic behavior $\Phi(x)\propto x$ for $x\ll 1$ and $\Phi(x)\propto x^{\alpha_\chi}$ for $x\gg 1$. Thus, the scaling properties are in line with dynamical ω/T scaling for the C and MCK fixed points. For the LM fixed point we find $\alpha_\chi=-1$ and a scaling form $\chi''(\omega)=T^{\alpha_\chi}\tilde{\Phi}(\omega/T^{1+\kappa})$, indicative of a weak-coupling fixed point and absence of hyperscaling. These results will be further addressed elsewhere [46]. The singlet-strength ϕ_s vs J at different T and at $V=0$ is shown in Fig. 2(b). The numerical data at $T\neq 0$ suggest that $\phi_s(J,T=0)$ is a continuous function of J. At the C fixed point we find that $\phi_s(J,T)$ as a function of J crosses for different values of T (for sufficiently low T).

Nonthermal steady states.—We consider a nonequilibrium setup where the two leads, initially decoupled from the impurity (for $t<t_0$), are held at chemical potentials $\mu_L=-\mu_R=|e|V/2$ ($|e|=1$ in the following). At $t=t_0$ the coupling between the leads and the impurity is turned on. A steady state is reached by sending $t_0\to-\infty$ so that any transient behavior will already have faded away at (finite) time t. The NESS fluctuation-dissipation ratio (FDR) for a dynamical observable $A(t,t')=A(t-t')$ is defined through $\mathrm{FDR}_A(\omega)=[A^>(\omega)+A^<(\omega)]/[A^>(\omega)-A^<(\omega)]$, where $A^{>/<}$ are the Fourier transforms of the greater/lesser components of A. At equilibrium, the fluctuation-dissipation theorem implies $\mathrm{FDR}_A(\omega)=\tanh(\beta\omega/2)^\zeta$ uniquely [with $\zeta=\pm 1$ for fermionic (+) and bosonic (−) operators]. For a generic out-of-equilibrium system, the functional form of the FDR differs from the equilibrium one. A frequency-dependent "effective temperature," $1/\beta^A_{\rm eff}(\omega)$, for the observable A can be defined by requiring that $\tanh[\beta^A_{\rm eff}(\omega)\omega/2]^\zeta=\mathrm{FDR}_A(\omega)$ [27,53]. Following Refs. [18,21,26] we define $T_{\rm eff}$ via FDR_χ through its asymptotic low-frequency behavior $T_{\rm eff}^{-1}=\lim_{\omega\to 0}\beta^\chi_{\rm eff}(\omega)$. In equilibrium $T_{\rm eff}=T$. On the other hand, a linear-in-V decoherence rate in the nonequilibrium relaxational regime near an interacting QCP is signaled by ω/V scaling [16]. In this case and at $T=0$ one expects $T_{\rm eff}=cV$, where c characterizes the underlying fixed point. We thus analyze $T/T_{\rm eff}$ vs V/T. Figure 2(c) shows the resulting $T/T_{\rm eff}$ as a function of V/T for the different fixed points computed for different values of V

and T. In the nonlinear regime, the scaling collapse for $T/T_{\rm eff}$ implies $T_{\rm eff} = cV$, where $1/c$ is the amplitude of the scaling curve in the nonlinear regime. A comparison of FDR_χ^{-1} with the equilibrium result for fixed point (C) is shown in Fig. 2(d). Even for the LM fixed point, where hyperscaling is violated, $T_{\rm eff} \sim V$ holds for $V \gg T$, see Fig. 2(c), top panel. It is, however, important to realize that the properties we see in terms of $T_{\rm eff}$ are a property of the flow towards the LM fixed point. Far from equilibrium and outside any scaling regime, χ is a function of ω, T, and V but near a fixed point $\chi(\omega, T, V)$ develops a scaling form in terms of a combination of ω, T, and V. This then raises the question how $T_{\rm eff}$ enters the scaling function and leads us to a remarkable result, see Figs. 3(b) and 3(c): The nonthermal steady-state scaling function of $\chi = \chi(\omega, T, V)$ when scaled in terms of $T_{\rm eff}$ recovers the equilibrium scaling function of that particular fixed point with $T_{\rm eff}$ replacing T. This not only turns out to be true for χ at each of the fixed points of the model but also holds for ϕ_s, a higher-order correlation function. We first consider the static susceptibility. Figure 3(a) shows the equilibrium scaling forms of $\chi'(0)^{-1}$ as a function of $T_{\rm eff}$ for different values of T and V for the LM, C, and MCK fixed points. The color coding reflects the values of T of the system. The equilibrium form (grey lines) is recovered even for $T_{\rm eff}/T \gg 1$.

A similar result can be obtained at finite ω: Fig. 3(b) shows the log derivative $\partial_{\ln\omega} \ln\chi''(\omega)$ as a function of $\omega/T_{\rm eff}$ for different values of T and V for the LM, C, and MCK fixed points. These should be compared with the equilibrium results, the underlying grey lines: The equilibrium scaling form is recovered by replacing T by $T_{\rm eff}$, both for $\omega \ll T_{\rm eff}$ and $\omega \gg T_{\rm eff}$ [54]. Note that $T_{\rm eff}$ is defined from the FDR of χ in the limit $\omega/T \to 0$. Therefore, the fact that the equilibrium scaling forms of $\chi'(0)$ and $\chi''(\omega)$ are reproduced for $T_{\rm eff}/T \gg 1$ and $\omega/T_{\rm eff} \gg 1$, respectively, is remarkable. Figure 3(c) depicts ϕ_s as a function of $T_{\rm eff}$ for different values of T and V. Again, the equilibrium scaling behavior (gray curves) is reproduced.

Unlike χ and ϕ_s, the conductance G depends on both pseudoparticle propagators G_f and G_B. One thus may wonder if $T_{\rm eff}$ can have any meaning for G. In Figs. 4(a) and 4(b) we show the conductance per channel $G = \mathcal{J}_P/V$ vs T and V, respectively. In the linear response regime $V, T \ll T_K(J)$ of the MCK phase, the current is proportional to the applied voltage $\mathcal{J}_P = G_0 V$. Outside of the scaling regime, i.e., for $V, T \gg T_K(J)$, G drops rapidly as V or T increase. The linear and nonlinear current-voltage characteristics display power-law behavior as $T, V \to 0$ [16,18]. Near C, i.e., for $J = J_c$, the relation between $\mathcal{J}_P$ and V is still linear, ($\mathcal{J}_P = G_c V$); however, the critical conductance G_c is much smaller than G_0. Figure 4(c) shows G vs $T_{\rm eff}$ for different values of T and V for the LM, C, and MCK fixed points. The grey curves are obtained by varying T at fixed V for the lowest value of V considered in our study, i.e., $V_{\rm min} = 10^{-8} D$. The temperature dependence of

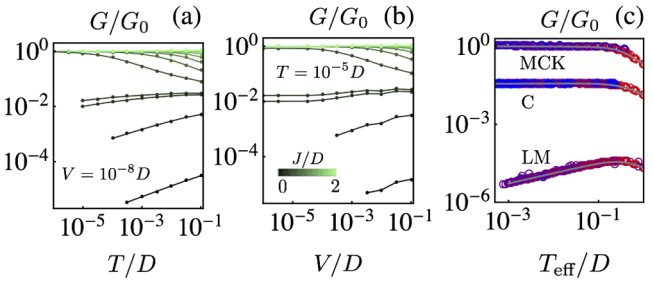

FIG. 4 (color online). Conductance G normalized to the MCK fixed point conductance $2\pi G_0 = 0.415$. (a) $G(T)$ vs T computed for the lowest nonzero value of V at different values of J (see color coding). (b) G vs V for fixed T. (c) $G = \mathcal{J}_P/V$ vs $T_{\rm eff}$ at different fixed points. The equilibrium form is given by the grey curves.

the linear response conductance is reproduced at all fixed points when the nonlinear conductance is taken as a function of $T_{\rm eff}$. This is true even for values of V several orders of magnitude larger than $V_{\rm min}$.

In conclusion, we have addressed the steady-state dynamics near unconventional quantum criticality. We found that in the scaling regime of all the fixed points considered, all observables studied (χ, ϕ_s, G) scale in terms of the same but fixed point specific effective temperature $T_{\rm eff}$. The local spin-spin correlation function χ and the singlet-strength ϕ_s assume their equilibrium scaling forms even far from equilibrium when scaled in terms of $T_{\rm eff}$, i.e., $T_{\rm eff}$ replacing T. A similar result relates the linear and nonlinear conductance. We note that in the (noninteracting) pseudogap resonant level model such behavior is absent [46]. It has been shown that the nonequilibrium current noise near quantum criticality in models possessing gravity duals appears thermal [55,56]. Our results imply that similar results hold for a larger class of quantum critical systems and quantities. The results reported here may thus help in identifying universality classes of unconventional quantum criticality. To what extent our results rely on locality needs to be further investigated.

Helpful discussions with K. Ingersent, A. Mitra, and Q. Si are gratefully acknowledged. P. Ribeiro acknowledges financial support from the Marie Curie International Reintegration Grant No. PIRG07-GA-2010-268172 and from FCT through the Contract Ref. IF/00347/2014/CP1214/CT0002 under the IF2014 program. S. Kirchner acknowledges partial support by the National Natural Science Foundation of China, Grant No. 11474250.

*stefan.kirchner@correlated-matter.com

[1] M. Eckstein, A. Hackl, S. Kehrein, M. Kollar, M. Moeckel, P. Werner, and F. Wolf, Eur. Phys. J. Spec. Top. **180**, 217 (2009).

[2] E. Arrigoni, M. Knap, and W. von der Linden, Phys. Rev. Lett. **110**, 086403 (2013).
[3] E. Muñoz, C. J. Bolech, and S. Kirchner, Phys. Rev. Lett. **110**, 016601 (2013).
[4] P. Werner, T. Oka, and A. J. Millis, Phys. Rev. B **79**, 035320 (2009).
[5] E. Gull, D. R. Reichman, and A. J. Millis, Phys. Rev. B **84**, 085134 (2011).
[6] G. Cohen, E. Gull, D. R. Reichman, A. J. Millis, and E. Rabani, Phys. Rev. B **87**, 195108 (2013).
[7] H. Aoki, N. Tsuji, M. Eckstein, M. Kollar, T. Oka, and P. Werner, Rev. Mod. Phys. **86**, 779 (2014).
[8] M. Schiró and M. Fabrizio, Phys. Rev. Lett. **105**, 076401 (2010).
[9] A. Rosch, Eur. Phys. J. B **85**, 6 (2012).
[10] H. T. M. Nghiem and T. A. Costi, Phys. Rev. B **90**, 035129 (2014).
[11] H. T. M. Nghiem and T. A. Costi, Phys. Rev. B **89**, 075118 (2014).
[12] A. Mitra, S. Takei, Y. B. Kim, and A. J. Millis, Phys. Rev. Lett. **97**, 236808 (2006).
[13] S. Diehl, A. Micheli, A. Kantian, B. Kraus, H. P. Büchler, and P. Zoller, Nat. Phys. **4**, 878 (2008).
[14] P. M. Hogan and A. G. Green, Phys. Rev. B **78**, 195104 (2008).
[15] C.-H. Chung, K. Le Hur, M. Vojta, and P. Wölfle, Phys. Rev. Lett. **102**, 216803 (2009).
[16] S. Kirchner and Q. Si, Phys. Rev. Lett. **103**, 206401 (2009).
[17] S. Takei, W. Witczak-Krempa, and Y. B. Kim, Phys. Rev. B **81**, 125430 (2010).
[18] P. Ribeiro, Q. Si, and S. Kirchner, Europhys. Lett. **102**, 50001 (2013).
[19] L. M. Sieberer, S. D. Huber, E. Altman, and S. Diehl, Phys. Rev. Lett. **110**, 195301 (2013).
[20] P. C. Hohenberg and B. I. Halperin, Rev. Mod. Phys. **49**, 435 (1977).
[21] P. C. Hohenberg and B. I. Shariman, Physica (Amsterdam) **37D**, 109 (1989).
[22] L. F. Cugliandolo, J. Kurchan, and L. Peliti, Phys. Rev. E **55**, 3898 (1997).
[23] P. Calabrese and A. Gambassi, J. Stat. Mech. (2004) P07013.
[24] J. Bonart, L. F. Cugliandolo, and A. Gambassi, J. Stat. Mech. (2012) P01014.
[25] L. F. Cugliandolo, J. Phys. A **44**, 483001 (2011).
[26] A. Mitra and A. J. Millis, Phys. Rev. B **72**, 121102 (2005).
[27] S. Kirchner and Q. Si, Phys. Status Solidi B **247**, 631 (2010).
[28] A. Caso, L. Arrachea, and G. S. Lozano, Phys. Rev. B **83**, 165419 (2011).
[29] P. Gegenwart, Q. Si, and F. Steglich, Nat. Phys. **4**, 186 (2008).
[30] J. X. Zhu, S. Kirchner, R. Bulla, and Q. Si, Phys. Rev. Lett. **99**, 227204 (2007).
[31] M. Vojta and R. Bulla, Phys. Rev. B **65**, 014511 (2001).
[32] J.-H. Chen, L. Li, W. G. Cullen, E. D. Williams, and M. S. Fuhrer, Nat. Phys. **7**, 535 (2011).
[33] A. Zhuravlev, I. Zharekeshev, E. Gorelov, A. I. Lichtenstein, E. R. Mucciolo, and S. Kettemann, Phys. Rev. Lett. **99**, 247202 (2007).
[34] L. G. G. V. Dias da Silva, N. P. Sandler, K. Ingersent, and S. E. Ulloa, Phys. Rev. Lett. **97**, 096603 (2006).
[35] D. Withoff and E. Fradkin, Phys. Rev. Lett. **64**, 1835 (1990).
[36] R. Bulla, T. Pruscke, and A. Hewson, J. Phys. Condens. Matter **9**, 10463 (1997).
[37] C. Gonzalez-Buxton and K. Ingersent, Phys. Rev. B **57**, 14254 (1998).
[38] D. E. Logan and M. T. Glossop, J. Phys. Condens. Matter **12**, 985 (2000).
[39] M. Vojta, Phys. Rev. Lett. **87**, 097202 (2001).
[40] K. Ingersent and Q. Si, Phys. Rev. Lett. **89**, 076403 (2002).
[41] M. T. Glossop and D. E. Logan, Europhys. Lett. **61**, 810 (2003).
[42] M. T. Glossop, G. E. Jones, and D. E. Logan, J. Phys. Chem. B **109**, 6564 (2005).
[43] L. Fritz, S. Florens, and M. Vojta, Phys. Rev. B **74**, 144410 (2006).
[44] M. T. Glossop, S. Kirchner, J. H. Pixley, and Q. Si, Phys. Rev. Lett. **107**, 076404 (2011).
[45] L. Fritz and M. Vojta, Rep. Prog. Phys. **76**, 032501 (2013).
[46] F. Zamani, P. Ribeiro, and S. Kirchner (unpublished).
[47] C.-H. Chung and K. Y.-J. Zhang, Phys. Rev. B **85**, 195106 (2012).
[48] M. Schiró, Phys. Rev. B **86**, 161101 (2012).
[49] A. Kaminski, Y. V. Nazarov, and L. I. Glazman, Phys. Rev. B **62**, 8154 (2000).
[50] O. Parcollet, A. Georges, G. Kotliar, and A. Sengupta, Phys. Rev. B **58**, 3794 (1998).
[51] See Supplemental Material at http://link.aps.org/supplemental/10.1103/PhysRevLett.115.220602 for details on the derivation and numerical evaluation of our results.
[52] P. Werner and M. Eckstein, Phys. Rev. B **86**, 045119 (2012).
[53] L. Foini, L. Cugliandolo, and A. Gambassi, Phys. Rev. B **84**, 212404 (2011).
[54] Similar results hold for the Keldysh component of χ.
[55] J. Sonner and A. G. Green, Phys. Rev. Lett. **109**, 091601 (2012).
[56] M. J. Bhaseen, B. Doyon, A. Lucas, and K. Schalm, Nat. Phys. **11**, 509 (2015).